Available online at www.sciencedirect.com
ScienceDirect
Journal of Sound and Vibration 310 (2008) 366–380
JOURNAL OF SOUND AND VIBRATION
www.elsevier.com/locate/jsvi

A study on the mode pair of a slightly asymmetric circular ring with multiple deviations

Han Gil Park[a], Jang Moo Lee[a], Yeon June Kang[a,*], Seock Hyun Kim[b]

[a]*Department of Mechanical and Aerospace Engineering, Seoul National University, San 56-1 Shinlim-dong, Kwanak-gu, Seoul, Republic of Korea*
[b]*Division of Mechanical and Mechatronics Engineering, Kangwon National University, Hyoja2-Dong 192-1, Chunchon-Si, Kangwon-Do 200-701, Republic of Korea*

Received 20 November 2006; received in revised form 3 August 2007; accepted 3 August 2007
Available online 29 September 2007

Abstract

This paper theoretically investigates the effect of multiple local deviations on the property of mode pair of a circular ring. The Laplace transform method is applied to the asymmetric ring with multiple local deviations. Multiple heavy side step functions are used to model the local deviations by using distributed mass, stiffness and thickness elements. The effect of multiple deviations on the change of the frequency of the mode pair is investigated. Beat frequency and configuration of the mode pair are investigated according to the amount and the position of the deviation. This study aims to explain the deviation effect on the beats of rings and bell type structures. The proposed analytical method can be used to control the beat characteristics of bell type structures.

1. Introduction

The effect of local deviation on the modal property of circular rings or shells in bell type structures, welded cylinders, ring gyroscopes, and rings with cracks is an interesting problem. In circular rings or cylindrical shells, slight asymmetry by local variation in mass, stiffness, or thickness produces a mode pair, which has slightly different frequency each other, and the interaction of the mode pair generates beating vibration and sound. These characteristics and artificial thickness variation are often applied to improve the beat characteristics of Oriental and Western bells [1,2]. Especially, in Korean bells, a particular section on the sound bow (ring type thick part) is ground after casting to control the beat period and beat strength. By proper reduction of the thickness of local elements, the modal property can be changed and the beating sound can be controlled.

In this study, we theoretically investigate the effect of multiple local deviations on the property of mode pair of a circular ring. We will examine how these local deviations can be used to control the beat property of bell type structures. The slight asymmetric effect of circular rings or cylindrical shells has been analyzed. Allaei et al. [3] investigated the free vibration behavior of rings with attached ground spring, attached torsional

*Corresponding author. Tel.: +82 2 880 1691; fax: +82 2 876 9493.
E-mail address: yeonjune@snu.ac.kr (Y.J. Kang).

0022-460X/$ - see front matter © 2007 Elsevier Ltd. All rights reserved.
doi:10.1016/j.jsv.2007.08.010

spring, and a point mass, by the receptance method. Cerep [4] used a harmonic approximation to derive the deflection function of a ring and used the Lagrange equation to analyze the in-plane vibration of circular rings on a tensionless foundation. Rossi [5] investigated the effect of non-uniform cross-section on the in-plane vibration of circular rings. He used the finite element method, in which explicit expressions for the stiffness and mass matrices were derived for generic elements of the ring's circular central axis.

To find an exact solution of a circular ring with small local deviation, Hong and Lee [6] developed a new method that could determine the natural frequency and mode shape without any use of trial functions or finite elements. They used the Laplace transform method for the eigenvalue analysis, and investigated the effect of a small local deviation on the natural frequencies and mode shapes of a circular ring. Kim et al. applied point receptance and line receptance to describe the impulse response of the ring stiffened cylindrical shell with slight asymmetry as a simplified bell type structure [7]. This approach is different from other analytical methods because it considers distributed deviation which other methods consider local deviation as an equivalent point (for ring) or line (for cylindrical shell) element. Hong and Lee's approach [6] is useful for explaining the beat characteristics of a bell type structure. In a Korean bell, clear beat and proper beat period are required to produce the long lasting hum and the fundamental tone [8]. To improve beat characteristics, local thickness is artificially controlled after casting.

In this paper, the Laplace transform method is expanded to the asymmetric ring with multiple local deviations. Multiple heavy side step functions are used to model the multiple deviations. The proposed method considers the deviations in terms of distributed mass, stiffness and thickness elements, while other methods in terms of the equivalent point mass or point spring. The effect of the multiple deviations on the frequency of the mode pair, the beat frequency and the configuration of the mode pair are discussed according to the amount and location of the deviations. The proposed analytical model can be used to control the beat characteristics of a bell type structure, which has similarity in the beat of the mode pair.

2. Equation of motion and analytic solution

The equation of motion of a circular ring is derived by reduction from Love's equations for shells. If the thickness of a ring is small relative to the radius, the circumferential inertia and shear deformations can be assumed to be negligible. In this case the equation of motion of a circular ring may be simplified as

$$\frac{\partial^3 M_b}{\partial\theta^3}+\frac{\partial M_b}{\partial\theta}=R^2\frac{\partial^2}{\partial t^2}\left[mv-\frac{\partial}{\partial\theta}(mu)\right], \tag{1}$$

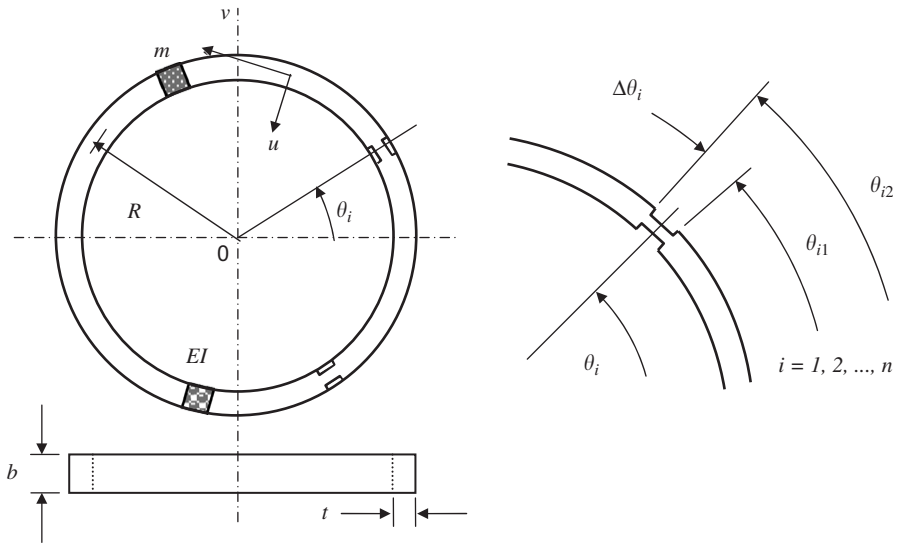

Fig. 1. Circular ring with multiple local deviations.

where R and m denote the radius and mass per unit length of a circular ring, and u and v are the radial (toward the center) and circumferential components of the displacement, respectively, as shown in Fig. 1. The relationship between the bending moment M_b and displacements u, v can be expressed as follows:

$$M_b = \frac{EI}{R^2}\left(\frac{\partial^2 u}{\partial\theta^2} + \frac{\partial v}{\partial\theta}\right). \tag{2}$$

From the inextensional approximation in which the extension of the reference surface is negligible, we can obtain the relation of u and v as Eq. (3), and the equation of motion of a circular ring can be simplified in the form of partial differential equation of variable u. The inextensional approximation is good for the natural modes where the transverse motion is dominant

$$u(\theta) = \frac{\partial v(\theta)}{\partial\theta}. \tag{3}$$

Now, consider a circular ring with multiple local deviations in stiffness and/or mass as shown in Fig. 1. Local deviations in stiffness and mass may be expressed in the form of heavy side step functions

$$EI = (EI)_u + \sum_{i=1}^{n}(EI)_i[H_{i1} - H_{i2}], \quad m = m_u + \sum_{i=1}^{n} m_i[H_{i1} - H_{i2}], \tag{4}$$

where $H_{i1} = H(\theta - \theta_{i1})$ and $H_{i2} = H(\theta - \theta_{i2})$ are the heavy side step functions. The subscript i denotes ith deviation, and $(EI)_i$ and m_i represent its added stiffness/mass properties, respectively. From Eqs. (1)–(4), the governing equation of motion for the circular ring with multiple local deviations is derived. Now EI and m are no longer constants but functions of the location θ.

Assuming harmonic time dependence, i.e., $v(\theta, t) = V(\theta)e^{j\omega t}$, Eq. (1) becomes

$$[V^{(6)} + 2V^{(4)} + V'' - \lambda(V'' - V)] - G_m + G_{EI} = 0, \tag{5}$$

where

$$G_m = \frac{\lambda}{m_u}\sum_{i=1}^{n} m_i[(V'' - V)(H_{i1} - H_{i2}) + V'(\delta_{i1} - \delta_{i2})],$$

$$G_{EI} = \frac{1}{(EI)_u}\sum_{i=1}^{n}(EI)_i[(V^{(6)} + 2V^{(4)} + V'')(H_{i1} - H_{i2}) + (3V^{(5)} + 4V''' + V')(\delta_{i1} - \delta_{i2}) + 3(V^{(4)} + V'')(\delta'_{i1} - \delta'_{i2}) + (V''' + V')(\delta''_{i1} - \delta''_{i2})],$$

where $\delta_{i1} = \delta(\theta - \theta_{i1})$ and $\delta_{i2} = \delta(\theta - \theta_{i2})$ are the derivatives of the heavy side step function, i.e., $(d/d\theta)[H(\theta)] = \delta(\theta)$. In this equation the primes denote derivatives with respect to θ and λ is the natural frequency parameter that is defined as

$$\lambda = \frac{m_u R^4 \omega^2}{(EI)_u}. \tag{6}$$

The continuity conditions of displacement and bending moments at $\theta = \theta_{i1}$ are

$$V(\theta_{i1}^+) = V(\theta_{i1}^-), \quad V'(\theta_{i1}^+) = V'(\theta_{i1}^-),$$
$$V'''(\theta_{i1}^+) + V'(\theta_{i1}^+) = \frac{(EI)_u}{(EI)_u + (EI)_a}[V'''(\theta_{i1}^-) + V'(\theta_{i1}^-)]. \tag{7}$$

The continuity conditions at $\theta = \theta_{i2}$ are obtained in a similar way.

To solve the eigenvalue problem, we take the Laplace transform of Eq. (5). At this time the continuity Eq. (7) is applied in the integration of non-homogeneous stiffness/mass terms which simplify the equation

as follows:

$$[s^6+2s^4+(1-\lambda)s^2-\lambda]\bar{V}(s)=[s^5+2s^3+(1-\lambda)s]V(0)+(s^4+2s^2+1-\lambda)V'(0)+(s^3+2s)V''(0)+(s^2+2)V'''(0)+sV^{(4)}(0)+V^{(5)}(0)+\lambda\sum_{i=1}^{n}M_i^*\,\mathrm{e}^{-s\theta_i}[s\hat{V}'(\theta_i)-\hat{V}(\theta_i)]-\sum_{i=1}^{n}(EI)_i^*\,\mathrm{e}^{-s\theta_i}(s^3+s)[\hat{V}'''(\theta_i)+\hat{V}'(\theta_i)], \tag{8}$$

where

$$\hat{V}^{(k)}(\theta_i)=\frac{1}{2}[V^{(k)}(\theta_{i1}^-)+V^{(k)}(\theta_{i2}^+)],\quad k=0,1,3,$$
$$M_i^*=\frac{m_a\,\Delta\theta}{m_u},\quad (EI)_i^*=\frac{(EI)_a\,\Delta\theta}{(EI)_u+(EI)_i}. \tag{9}$$

Here $\hat{V}(\theta_i)$ is a mean displacement value in the ith non-homogeneous section, and M_i^* and $(EI)_i^*$ are non-dimensional parameters of mass/stiffness changes.

The solution of the circular ring with deviations can be obtained from the inverse Laplace transform of Eq. (8). When $\bar{V}(s)$ is expressed as the sum of homogeneous and non-homogeneous solution, i.e., $\bar{V}(s)=\bar{F}_a(s)+\sum_{i=1}^{n}\mathrm{e}^{-s\theta_i}\bar{F}_i(s)$, the inverse transform of Eq. (8) can be expressed as

$$V(\theta)=L^{-1}\{\bar{F}_a(s)\}+\sum_{i=1}^{n}H(\theta-\theta_i)[L^{-1}\{\bar{F}_i(s)\}]_{\theta=\theta-\theta_i}. \tag{10}$$

Assuming $V(\theta)$ to have simple poles at $s=\pm Z_1$, $\pm Z_2$ and $\pm Z_3$, i.e., $s^6+2s^4+(1-\lambda)s^2-\lambda=(s+Z_1)(s-Z_1)(s+Z_2)(s-Z_2)(s+Z_3)(s-Z_3)=0$, the inverse transform can then be obtained by the residue theorem:

$$V(\theta)=\sum_{i=1}^{n}\sum_{j=1}^{3}[A_j\cosh(Z_j\theta)+B_j\sinh(Z_j\theta)]+\sum_{i=1}^{n}\sum_{j=1}^{3}H(\theta-\theta_i)[C_{ij}\cosh\{Z_j(\theta-\theta_i)\}+D_{ij}\sinh\{Z_j(\theta-\theta_i)\}], \tag{11}$$

where

$$A_j=\frac{1}{Q_j}[\{Z_j^5+2Z_j^3+(1-\lambda)Z_j\}V(0)+(Z_j^3+2Z_j)V''(0)+Z_jV^{(4)}(0)],$$
$$B_j=\frac{1}{Q_j}[(Z_j^4+2Z_j^2+1-\lambda)V'(0)+(Z_j^2+2)V'''(0)+V^{(5)}(0)],$$
$$C_{ij}=\frac{Z_j}{Q_j}\lambda M_i^*\hat{V}'(\theta_i)-\frac{Z_j^3+Z_j}{Q_j}(EI)_i^*[\hat{V}'''(\theta_i)+\hat{V}'(\theta_i)],$$
$$D_{ij}=-\frac{1}{Q_j}\lambda M_i^*\hat{V}(\theta_i),$$
$$Q_j=3Z_j^5+4Z_j^3+(1-\lambda)Z_j,\quad j=1,\,2,\,3. \tag{12}$$

To obtain the eigenvalues and eigenvectors, we used the matching boundary conditions. The displacement and its derivatives must be continuous at $\theta=0$ and 2π, i.e.,

$$V^{(k)}(0)=V^{(k)}(2\pi),\quad k=0,1,\ldots,5. \tag{13}$$

If we apply the matching boundary conditions to Eqs. (11)–(13), the following equations are acquired:

$$\sum_{j=1}^{3}Z_j^kG_{jr}=0,\quad k=0,1,\ldots,5,\quad r=\begin{cases}1 & \text{(even number } k),\\ 2 & \text{(odd number } k),\end{cases} \tag{14}$$

where

$$G_{j1} = (a_j - 1)A_j + b_j B_j + \sum_{i=1}^{n}(c_{ij}C_{ij} + d_{ij}D_{ij}),\ G_{j2} = b_j A_j + (a_j - 1)B_j + \sum_{i=1}^{n}(d_{ij}C_{ij} + c_{ij}D_{ij}),$$

$$a_j = \cosh(2\pi Z_j), \quad b_j = \sinh(2\pi Z_j), \quad c_{ij} = \cosh\{Z_j(2\pi - \theta_i)\}, \quad d_{ij} = \sinh\{Z_j(2\pi - \theta_i)\}.$$

Because we assumed the simple poles, Z_j's are different from one another, and all G_{jr} should be zero to satisfy Eq. (14). This relationship can then be obtained:

$$\begin{bmatrix} a_j - 1 & b_j \\ b_j & a_j - 1 \end{bmatrix} \begin{Bmatrix} A_j \\ B_j \end{Bmatrix} = -\begin{Bmatrix} \sum_{i=1}^{n}(c_{ij}C_{ij} + d_{ij}D_{ij}) \\ \sum_{i=1}^{n}(d_{ij}C_{ij} + c_{ij}D_{ij}) \end{Bmatrix}. \tag{15}$$

From the above relationship, A_j and B_j can be expressed as a function of C_{ij} and D_{ij}. The solutions are then expressed as

$$V(\theta) = -\sum_{i=1}^{n}\sum_{j=1}^{3}\frac{1}{2\sinh(\pi Z_j)}[C_{ij}\ \sinh\{Z_j(\theta - \theta_i + \pi)\} + D_{ij}\ \cosh\{Z_j(\theta - \theta_i + \pi)\}]$$
$$+ \sum_{i=1}^{n}\sum_{j=1}^{3} H(\theta - \theta_i)[C_{ij}\ \cosh\{Z_j(\theta - \theta_i)\} + D_{ij}\ \sinh\{Z_j(\theta - \theta_i)\}],$$

$$U(\theta) = \frac{\partial}{\partial\theta} V(\theta). \tag{16}$$

We can get the value of $\hat{V}^{(k)}(\theta_i)$ from Eqs. (9), (12) and (16). Substituting Eq. (12) into Eq. (16) allows us to evaluate Eq. (9), and we can get the characteristic equation from those equations. They are

$$\sum_{i=1}^{n}[{}_0A_{ki}\hat{V}(\theta_i) + {}_1A_{ki}\hat{V}'(\theta_i) + {}_3A_{ki}\hat{V}'''(\theta_i)] = 0,$$
$$\sum_{i=1}^{n}[{}_0B_{ki}\hat{V}(\theta_i) + {}_1B_{ki}\hat{V}'(\theta_i) + {}_3B_{ki}\hat{V}'''(\theta_i)] = 0, \quad (k = 1, 2, \ldots, n),$$
$$\sum_{i=1}^{n}[{}_0C_{ki}\hat{V}(\theta_i) + {}_1C_{ki}\hat{V}'(\theta_i) + {}_3C_{ki}\hat{V}'''(\theta_i)] = 0, \tag{17}$$

where

for $1 \leqslant i \leqslant k - 1$:

$${}_0A_{ki} = \sum_{j=1}^{3} K(F + S), \quad {}_1A_{ki} = \sum_{j=1}^{3} I(E + C), \quad {}_3A_{ki} = \sum_{j=1}^{3} J(E + C),$$
$${}_0B_{ki} = \sum_{j=1}^{3} Z_j K(E + C), \quad {}_1B_{ki} = \sum_{j=1}^{3} Z_j I(F + S), \quad {}_3B_{ki} = \sum_{j=1}^{3} Z_j J(F + S),$$
$${}_0C_{ki} = \sum_{j=1}^{3} Z_j^3 K(E + C), \quad {}_1C_{ki} = \sum_{j=1}^{3} Z_j^3 I(F + S), \quad {}_3C_{ki} = \sum_{j=1}^{3} Z_j^3 J(F + S),$$

for $i = k$:

$${}_0A_{ki} = \sum_{j=1}^{3}(FK) - 1, \quad {}_1A_{ki} = \sum_{j=1}^{3} I(E + 0.5), \quad {}_3A_{ki} = \sum_{j=1}^{3} J(E + 0.5),$$
$${}_0B_{ki} = \sum_{j=1}^{3} Z_j K(E + 0.5), \quad {}_1B_{ki} = \sum_{j=1}^{3}(Z_j FI) - 1, \quad {}_3B_{ki} = \sum_{j=1}^{3}(Z_j FJ),$$
$${}_0C_{ki} = \sum_{j=1}^{3} Z_j^3 K(E + 0.5), \quad {}_1C_{ki} = \sum_{j=1}^{3}(Z_j^3 FI), \quad {}_3C_{ki} = \sum_{j=1}^{3}(Z_j^3 FJ) - 1,$$

for $k+1 \leqslant i \leqslant n$:

$$
{}_0A_{ki} = \sum_{j=1}^{3}(FK), \quad {}_1A_{ki} = \sum_{j=1}^{3}(EI), \quad {}_3A_{ki} = \sum_{j=1}^{3}(EJ),
$$

$$
{}_0B_{ki} = \sum_{j=1}^{3}(Z_jEK), \quad {}_1B_{ki} = \sum_{j=1}^{3}(Z_jFI), \quad {}_3B_{ki} = \sum_{j=1}^{3}(Z_jFJ),
$$

$$
{}_0C_{ki} = \sum_{j=1}^{3}(Z_j^3EK), \quad {}_1C_{ki} = \sum_{j=1}^{3}(Z_j^3FI), \quad {}_3C_{ki} = \sum_{j=1}^{3}(Z_j^3FJ).
$$

At all non-homogeneous section i's,

$$
I = \frac{Z_j}{Q_j}[\lambda M_i^* - (Z_j^2+1)(EI)_i^*], \quad J = -\frac{Z_j^3+Z_j}{Q_j}(EI)_i^*, \quad K = -\frac{1}{Q_j}\lambda M_i^*,
$$

$$
E = -\frac{1}{2}\left[\frac{\sinh(\Delta_{ki}Z_j)}{\tanh(\pi Z_j)} + \cosh(\Delta_{ki}Z_j)\right], \quad F = -\frac{1}{2}\left[\frac{\cosh(\Delta_{ki}Z_j)}{\tanh(\pi Z_j)} + \sinh(\Delta_{ki}Z_j)\right],
$$

$$
S = \sinh(\Delta_{ki}Z_j), \quad C = \cosh(\Delta_{ki}Z_j), \quad \Delta_{ki} = \theta_k - \theta_i.
$$

Eq. (17) can be expressed in a simple matrix form:

$$
\mathbf{Mx} = \begin{bmatrix} \mathbf{M}_{11} & \mathbf{M}_{12} & \cdots & \mathbf{M}_{1n} \\ \mathbf{M}_{21} & \mathbf{M}_{22} & \cdots & \mathbf{M}_{2n} \\ \vdots & \vdots & & \vdots \\ \mathbf{M}_{n1} & \mathbf{M}_{n2} & \cdots & \mathbf{M}_{nn} \end{bmatrix} \begin{Bmatrix} \mathbf{x}_1 \\ \mathbf{x}_2 \\ \vdots \\ \mathbf{x}_n \end{Bmatrix} = 0, \tag{18}
$$

where

$$
\mathbf{M}_{ki} = \begin{bmatrix} {}_0\mathbf{A}_{ki} & {}_1\mathbf{A}_{ki} & {}_3\mathbf{A}_{ki} \\ {}_0\mathbf{B}_{ki} & {}_1\mathbf{B}_{ki} & {}_3\mathbf{B}_{ki} \\ {}_0\mathbf{C}_{ki} & {}_1\mathbf{C}_{ki} & {}_3\mathbf{C}_{ki} \end{bmatrix}, \quad \mathbf{x}_k = \begin{Bmatrix} \hat{\mathbf{V}}(\theta_k) \\ \hat{\mathbf{V}}'(\theta_k) \\ \hat{\mathbf{V}}'''(\theta_k) \end{Bmatrix}.
$$

For a non-trivial solution, the determinant of matrix $\mathbf{M}$ should be zero. The characteristic equation for obtaining the eigenvalues of the circular ring with multi local deviation is given as

$$
\det(\mathbf{M}) = 0. \tag{19}
$$

Since the Z_j's are roots of $s^6 + 2s^4 + (1-\lambda)s^2 + \lambda = 0$, at least one of the Z_j's is imaginary. If we let $Z_1 = j\alpha$ (α is a real number), the natural frequency parameter λ comes to

$$
\lambda = \frac{\alpha^2(\alpha^2-1)^2}{\alpha^2+1} \tag{20}
$$

and other two roots are evaluated using following equations:

$$
Z_2^2 = \frac{1}{2}\left[(\alpha^2-2) + \sqrt{(\alpha^2-2)^2 - \frac{4\lambda}{\alpha^2}}\right], \quad Z_3^2 = \frac{1}{2}\left[(\alpha^2-2) - \sqrt{(\alpha^2-2)^2 - \frac{4\lambda}{\alpha^2}}\right]. \tag{21}
$$

We can obtain α's and thus λ's from Eqs. (19)–(21) and the mode shapes can be obtained easily from Eq. (16).

3. Analysis of results and verification

3.1. Symmetric ring without local deviation

Before the analysis of the ring with deviation, we compared the natural frequencies by the proposed method with those by the finite element analysis for an axisymmetric ring. The dimensions and properties of a circular

Table 1
Dimensions and properties of the circular ring

Dimension		Property	
Diameter (D)	2040 mm	Young's modulus (E)	206 GPa
Thickness (t)	131 mm	Density (ρ)	7860 kg/m^3
Width (b)	100 mm		

Table 2
Natural frequencies of the circular ring with one local mass deviation (one mass element at $\theta = 22.5^\circ$, $\Delta\theta = 9^\circ$, $m_i = 0.3m_u$)

Mode (n)	$f_{\text{th\_0}}$ (Hz)	f_{th} (Hz)	$f_{\text{FEM\_0}}$ (Hz)	f_{FEM} (Hz)	Difference (%)
2-L	79.16	78.70	78.60	78.14	0.72
2-H		79.05		78.48	0.73
3-L	223.91	222.43	219.85	218.43	1.83
3-H		223.74		219.65	1.86
4-L	429.33	426.39	415.07	412.35	3.40
4-H		429.14		414.76	3.47
5-L	694.32	689.52	658.60	654.28	5.39
5-H		694.12		658.08	5.48

ring are listed in Table 1. The dimensions of the ring has been determined by considering the maximum thickness (sound bow) of a large Korean bell. We used the commercial FEM code, ANSYS for FE analysis and the element used in FEA is SOLID 45. The eigenvalue problem formulated within the FEM for the vibration analysis is solved by the reduced subspace method. Table 2 shows the computed results.

On the other hand, for the symmetric ring the radial component of the mode function is represented as follows [9]:

$$u_n(\theta) = U \cos n(\theta + \theta_o + \gamma), \quad \gamma = 0, \pi/2n, \quad (n = 2, 3, \ldots). \tag{22}$$

where n denotes the mode number of the symmetric ring. Hong and Lee [6] have shown that the analytical mode of Eq. (16) becomes Eq. (22), if the local deviation becomes zero, i.e., for a symmetric ring.

Natural frequencies obtained by both methods are in very good agreement in low order modes, but somewhat different in high order modes. This difference is caused by the neglect of the shear deformation, rotary inertia, thickness motion in the analytical solution. We checked that the difference in the results between the two methods becomes small as the ratio of radial thickness to radius decreases. Even though the ratio exceeds 0.1 as in a Korean bell, the calculated frequencies of $n = 2$ and 3 modes, that correspond to the hum and the fundamental tone are, respectively, in good agreement between the two methods.

3.2. Asymmetric ring with local mass deviations

3.2.1. One local mass element

Table 2 shows the frequency shift by adding one asymmetric mass element. Mass density is increased by 30% for the 9° length element positioned at $\theta = 22.5^\circ$. Here, $f_{\text{th\_0}}$ represents theoretical solution with no deviation and f_{th} represents theoretical solution with deviations. Likewise, $f_{\text{FEM\_0}}$ stands for numerical solution with no deviation and f_{FEM} stands for numerical solution with deviation. Lastly difference is expressed by $(f_{\text{th}} - f_{\text{FEM}})/f_{\text{FEM}}$.

As an important application, that position is often ground after casting to generate clear beat in the Korean bell [9]. The mode pairs denoted by n-L and n-H, respectively, have slightly different frequencies, but their mode shapes are almost equal to those of the symmetric ring. Δf_{th} and Δf_n mean the frequency shift from the original axisymmetric state. Frequency difference in each mode pair generates beating. The results of the frequency shift obtained by the two methods for each mode are in good agreement.

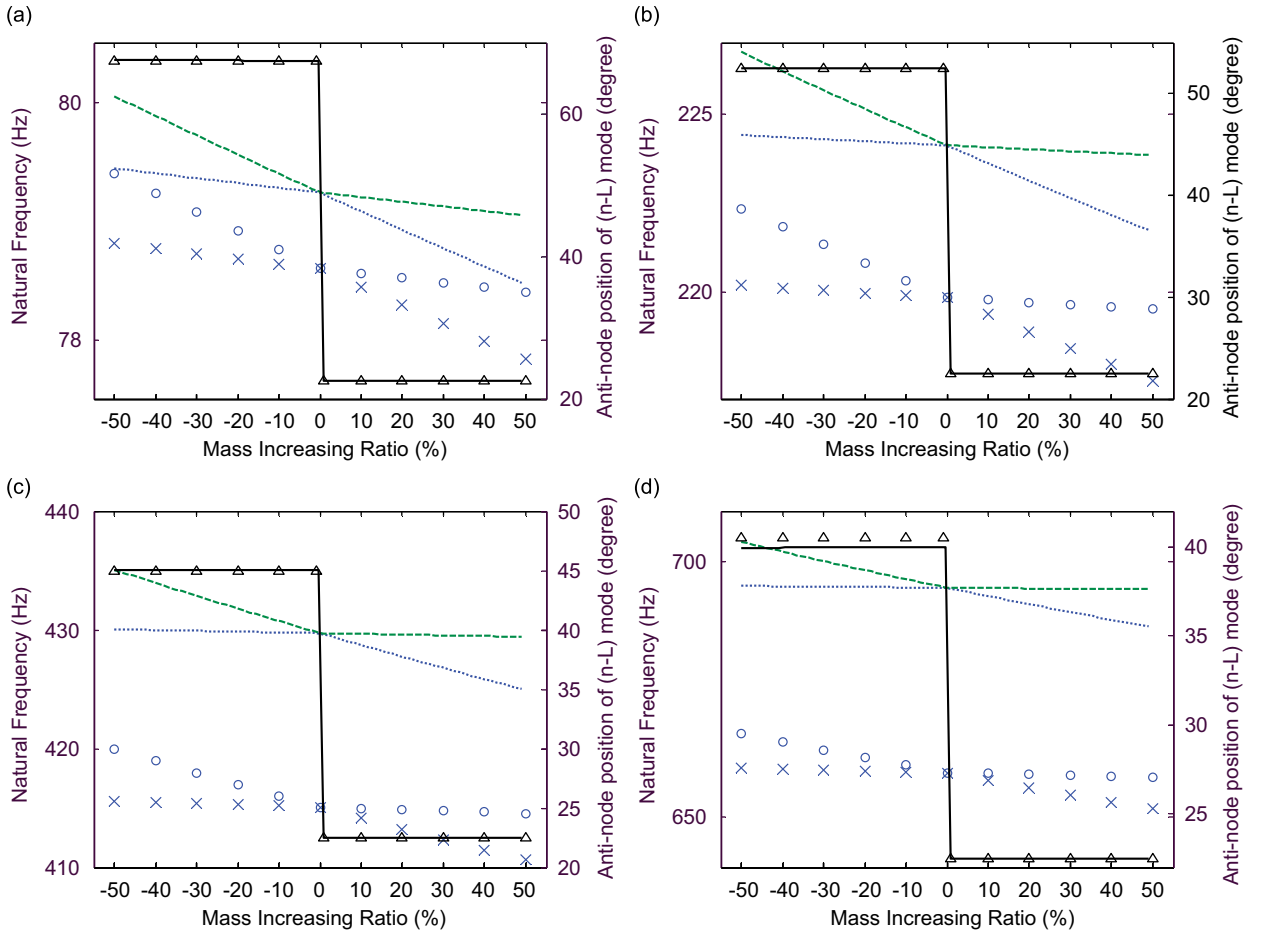

Fig. 2. Natural frequencies and anti-node position for one mass element: (a) $n = 2$ mode; (b) $n = 3$ mode; (c) $n = 4$ mode; and (d) $n = 5$ mode. (– – $(n\text{–H})_{\text{theory}}$, ····: $(n\text{–L})_{\text{theory}}$, —: anti-node position of $(n\text{–L})_{\text{theory}}$, ○: $(n\text{–H})_{\text{FEM}}$, X: $(n\text{–L})_{\text{FEM}}$, △: anti-node position of $(n\text{–L})_{\text{FEM}}$).

Fig. 2 shows the variation of the amount of frequency shift and anti-nodal line position with the increase of the mass effect. In the figures, zero mass increasing ratio stands for the axisymmetry of the ring. In case of the positive mass increasing ratio, the natural frequency decreases as the mass effect increases.

Frequency shift is remarkable in the n-L mode since it has the anti-node at the element position (i.e., at $\theta = 22.5^\circ$), but is very small in the n-H mode since the node passes the position of the mass element. The anti-node of the n-L mode (the node of n-H mode) positions itself at every $90^\circ/n$ from 22.5°. Negative mass increasing ratio represents the mass reduction of the local element. Natural frequency increases with the negative mass increasing ratio. The node of the n-L mode moves to the element position and naturally that position becomes the anti-node of the n-H mode. This configuration of the nodes agrees well with those in other studies [2,8].

In the figures, the difference of the n-H frequency and n-L frequency, i.e., the beat frequency is more meaningful than the frequencies themselves. Considering the initial deviation in the axisymmetric ring (Table 2), Fig. 2 shows good agreement for the changing tendency of the beat frequency.

3.2.2. Two local mass elements

Table 3 shows the natural frequencies when two local mass deviations are placed at 67.5° and 90° locations, respectively, and the length of each element is 9°. The amount of frequency shift Δf obtained by the two

Table 3
Natural frequencies of the asymmetric ring with two local mass deviations (deviations at $\theta_1 = 67.5^\circ$, $\theta_2 = 90^\circ$; $\Delta\theta_{1,2} = 9^\circ$, $m_1 = 0.2m_u$, $m_2 = 0.3m_u$)

Mode (n)	f_{th_0} (Hz)	f_{th} (Hz)	f_{FEM_0} (Hz)	f_{FEM} (Hz)	Difference (%)
2-L	79.16	78.47	78.60	77.91	0.72
2-H		78.89		78.33	0.71
3-L	223.91	222.08	219.85	218.07	1.84
3-H		223.02		218.95	1.86
4-L	429.33	426.28	415.07	412.16	3.43
4-H		427.18		412.95	3.44
5-L	694.32	688.52	658.60	653.30	5.39
5-H		691.70		655.85	5.47

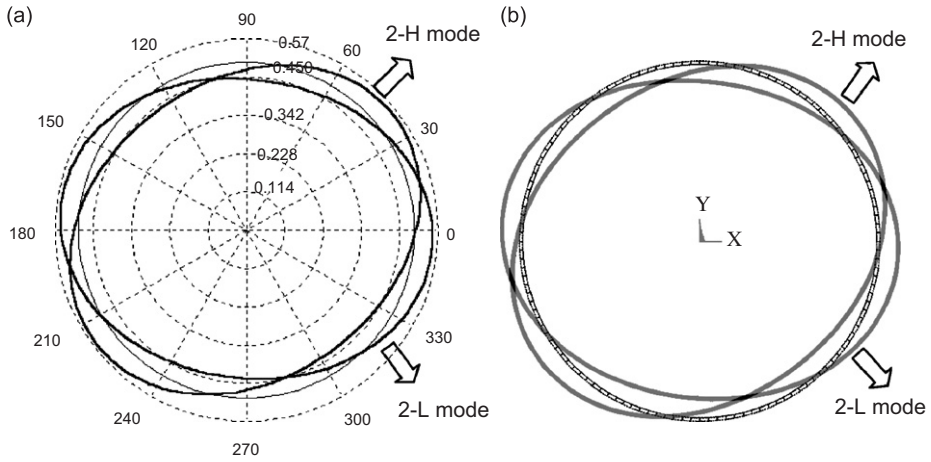

Fig. 3. $n = 2$ mode of the circular ring (deviations at $\theta = 67.5^\circ$, 90°; $m_1 = 0.2m_u$, $m_2 = 0.3m_u$): (a) theoretical mode and (b) FEM.

methods also agrees very well. As shown in Figs. 3 and 4, node and anti-node positions exactly coincide in both two methods.

3.3. Asymmetric ring with local stiffness deviations

3.3.1. One local stiffness element

We investigated the frequency shift due to the decrease of the stiffness of one element located at 22.5°. The element length was 9° as in the previous case. Table 4 shows the frequency shift by the 30% of stiffness reduction ratio. As in the case of the mass increase, the anti-node of the n-L mode (i.e., node of n-H mode) passes the reduced stiffness element. The beat frequencies by two methods were in good agreement, although a small difference was observed in the higher order modes. The frequency shift due to stiffness reduction ratio is shown in Fig. 5.

Compared with the case of the local mass increment, the natural frequency of the lower mode decreased rapidly with the stiffness reduction and the frequency of the higher mode hardly changed. The location of the L mode anti-node was fixed, bearing no relation to the stiffness reduction ratio. As a result the local stiffness reduction increased the beating frequencies better than the local mass increment did, and the tendency of the variation of frequency between the two methods was similar.

3.3.2. Two asymmetric stiffness elements

The natural frequencies and mode shapes were calculated when two local stiffness deviations were made at 60° and 90° shifts. Table 5 shows the results. From the comparison of the calculated results obtained by the

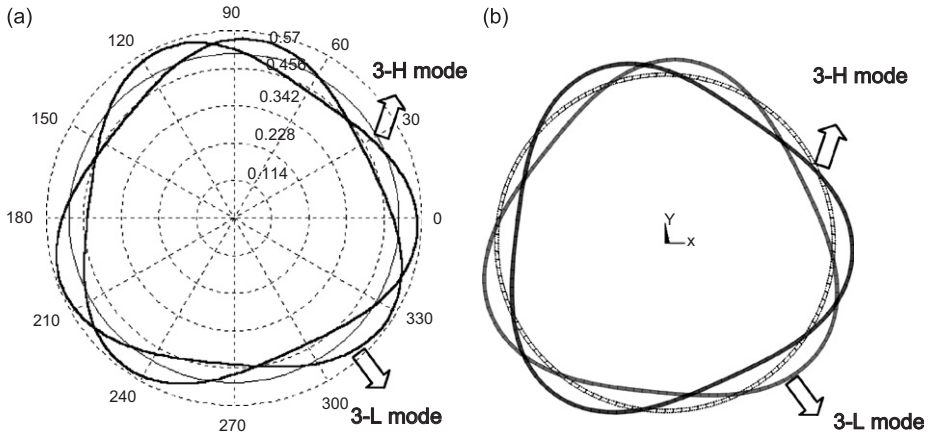

Fig. 4. $n = 3$ mode of the circular ring (deviations at $\theta = 67.5^\circ$, 90°; $m_1 = 0.2m_u$, $m_2 = 0.3m_u$): (a) theoretical mode and (b) FEM.

Table 4
Natural frequencies of the circular ring with one local stiffness deviation (deviations at $\theta = 22.5^\circ$, $\Delta\theta = 9^\circ$, $EI_i = -0.3EI_u$)

Mode (n)	$f_{\text{th\_0}}$ (Hz)	f_{th} (Hz)	$f_{\text{FEM\_0}}$ (Hz)	f_{FEM} (Hz)	Difference (%)
2-L	79.16	78.350	78.60	77.812	0.69
2-H		79.164		78.581	0.74
3-L	223.91	221.64	219.85	217.74	1.79
3-H		223.91		219.73	1.90
4-L	429.33	425.06	415.07	411.29	3.35
4-H		429.33		414.71	3.53
5-L	694.32	687.50	658.60	652.93	5.29
5-H		694.32		657.75	5.56

two methods, we could verify that the proposed analytic method also could give reasonably accurate natural frequencies for multiple stiffness deviations. The mode shapes between the analytic method and the finite element analysis were coincident as in the case of local mass deviations. Especially, the 3-L and 3-H mode pairs showed almost the same frequency because the stiffness deviations are located at 30° interval, and the two deviation elements became the nodal points of the mode pair. This indicates that beat frequency may be controlled by the mode with proper choice of the deviation positions.

3.4. Asymmetric ring with local thickness deviations

3.4.1. One local thickness element

Thickness deviation simultaneously incorporates the effect of mass and stiffness deviations. In Fig. 1, if we set the thickness reduction to t at the section of $\theta_1 < \theta < \theta_2$ for a circular ring with the initial thickness h, the local mass and stiffness variations are as follows:

$$M = M_0 \frac{h-t}{h} \text{ and } EI = EI_0 \left(\frac{h-t}{h}\right)^3 \quad \text{at } \theta_1 < \theta < \theta_2.$$

We may expect that the stiffness reduction would have much more effect than the mass reduction since the stiffness is proportional to the cube of the thickness ratio. This thickness reduction effect is usually applied to change the beating frequencies of a Korean bell after casting.

The thickness at the 22.5° position is often reduced to generate a clear beat in a Korean bell. Since the 0° position becomes the mid-point of the anti-nodes of the 2-L mode and 2-H mode, striking the 0° position

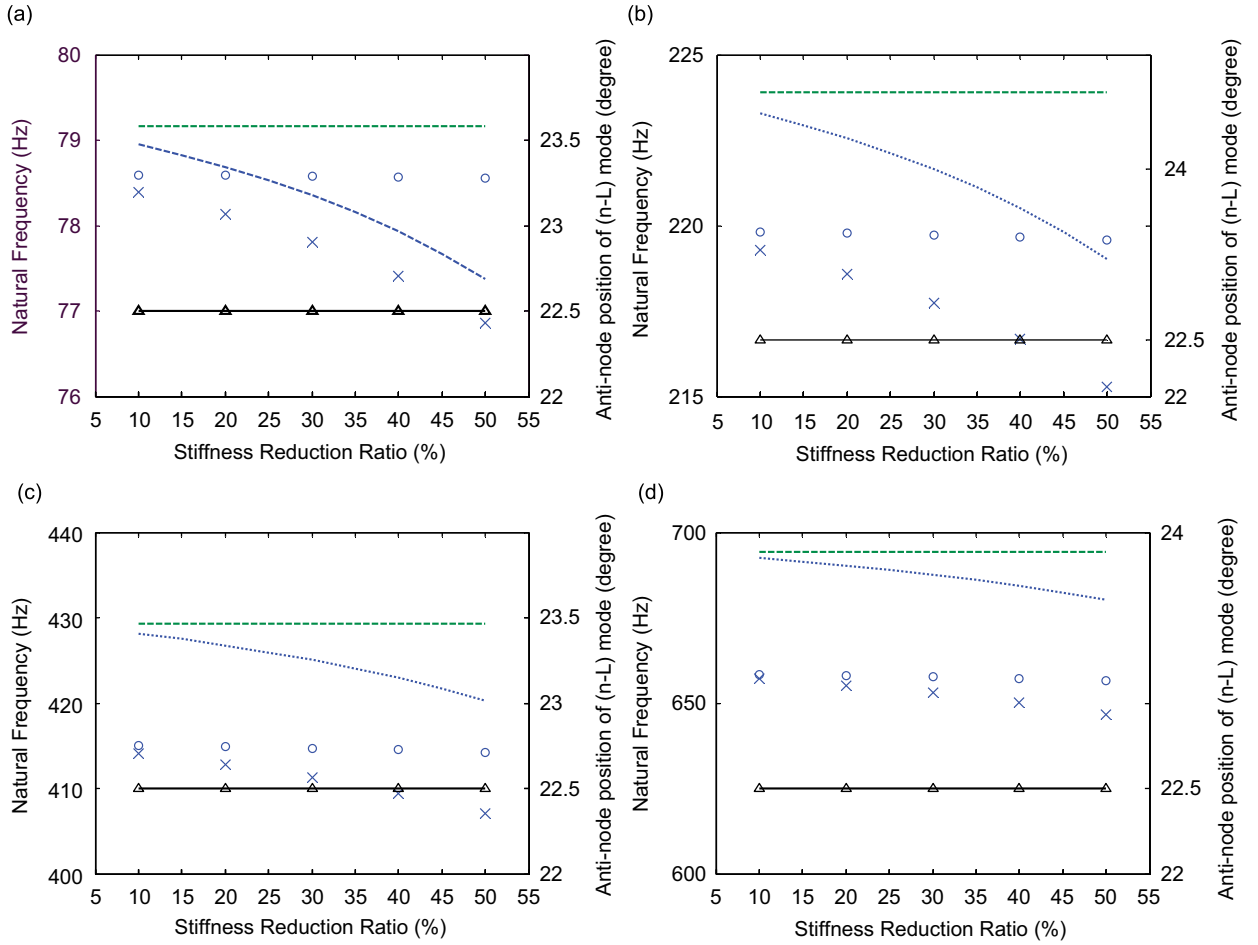

Fig. 5. Natural frequencies and anti-node position for one stiffness element (deviations at $\theta = 22.5°$, $\Delta\theta = 9°$, $EI_i = 0.1EI_u$–$0.5EI_u$): (a) $n = 2$ mode; (b) $n = 3$ mode; (c) $n = 4$ mode and (d) $n = 5$ mode. (– – (n–H)$_{\text{theory}}$, ····: (n–L)$_{\text{theory}}$, —: anti-node position of (n–L)$_{\text{theory}}$, ○: (n–H)$_{\text{FEM}}$, X: (n–L)$_{\text{FEM}}$, △: anti-node position of (n–L)$_{\text{FEM}}$).

Table 5
Natural frequencies of the circular ring with local deviations in stiffness (deviations at $\theta = 60°$, $90°$; $\Delta\theta = 9°$, $EI_i = -0.2EI_u$)

Mode (n)	$f_{\text{th\_0}}$ (Hz)	f_{th} (Hz)	$f_{\text{FEM\_0}}$ (Hz)	f_{FEM} (Hz)	Difference (%)
2-L	79.16	78.46	78.60	77.91	0.71
2-H		78.92		78.34	0.74
3-L	223.91	222.52	219.85	218.49	1.84
3-H		222.59		218.55	1.85
4-L	429.33	425.37	415.07	411.46	3.38
4-H		428.08		413.66	3.49
5-L	694.32	686.50	658.60	652.03	5.29
5-H		693.77		657.24	5.56

excites two modes equally and a clear beat is generated. We considered the frequency shift by one thickness element that was located at 22.5° and 9° long. As previously stated, the stiffness reduction effect and the mass reduction effect occur simultaneously. As a result, Fig. 6 shows that the thickness reduction decreases the

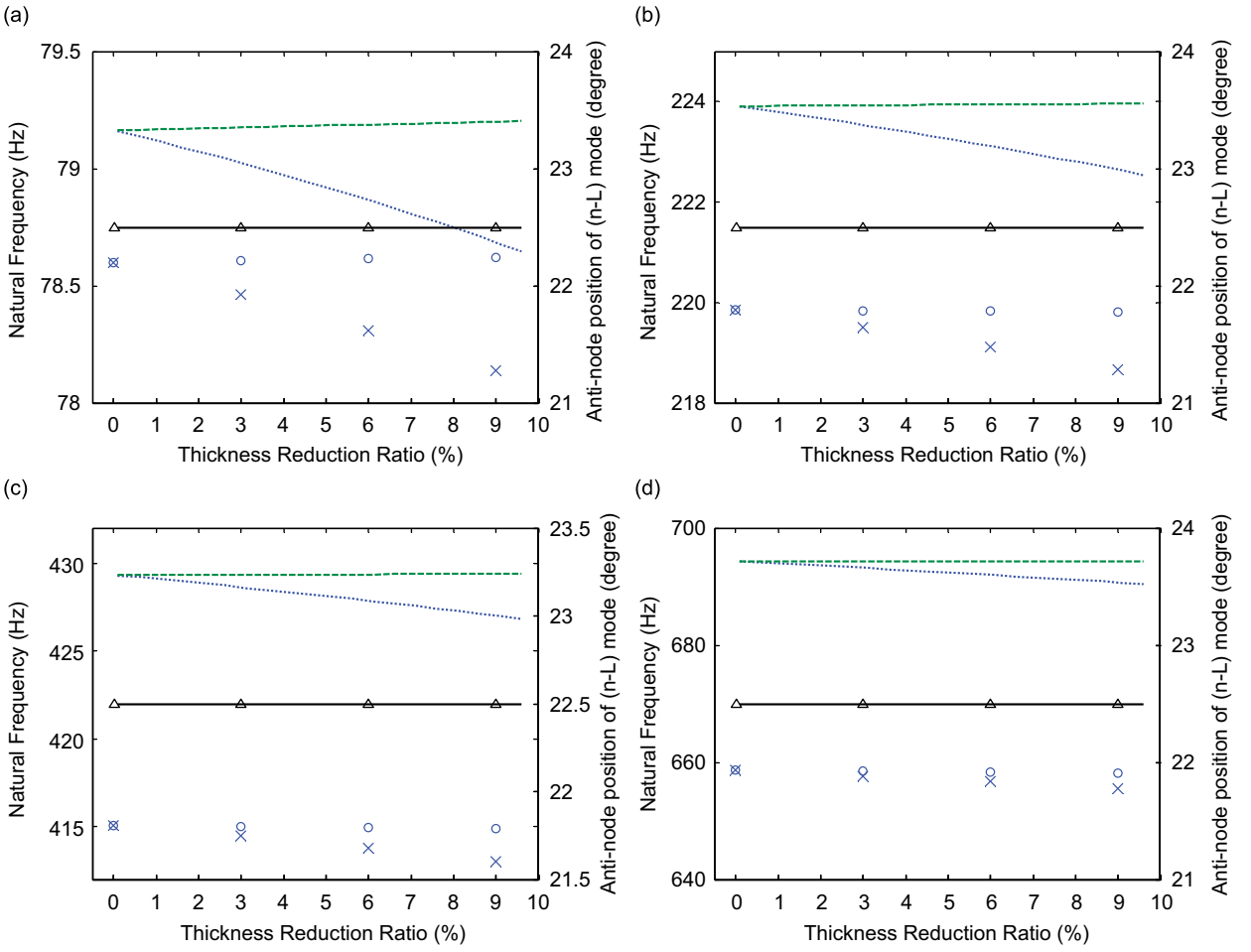

Fig. 6. Natural frequencies and anti-node position for one thickness element (deviations at $\theta = 22.5^\circ$; $\Delta\theta = 9^\circ$, t_i: 0–0.1t): (a) $n = 2$ mode; (b) $n = 3$ mode; (c) $n = 4$ mode; and (d) $n = 5$ mode. (– – (n–H)$_{\text{theory}}$, ····: (n–L)$_{\text{theory}}$, —: anti-node position of (n–L)$_{\text{theory}}$, ○: (n–H)$_{\text{FEM}}$, X: (n–L)$_{\text{FEM}}$, △: anti-node position of (n–L)$_{\text{FEM}}$).

natural frequency of the n-L mode and the anti-node of the L mode is fixed at 22.5°, which is similar to the case of stiffness reduction. The fact that the anti-node of the 2-L mode (i.e., the node of 2-H mode) passes the 22.5° position means that the anti-node of the 2-H mode passes the −22.5° position.

The n-H mode does not show the frequency reduction, rather the natural frequency increases slightly in the 2-H mode. It seems that the mass and stiffness effects are almost equal when the thickness is reduced around the node. In Fig. 6, we can see that the results between the proposed method and the finite element analysis show very similar tendency in the change of the natural frequency.

3.4.2. *Two local thickness elements*

In the tuning of a bell structure, the thickness reduction of one position may shorten the life of the bell since the stress by striking is concentrated on the local deviation. It is desirable to tune the beat characteristics by reducing the thickness at more than 2 positions on the bell. We studied the shift of the natural frequency by two thickness elements, which are located at 22.5° and 112.5°, respectively, and both are 9° long.

Two thickness elements are 90° apart from each other. For the $n = 2$ mode, both elements become the anti-nodes of the 2-L mode. Frequency decrease effect by the two elements is doubled that of the case of one

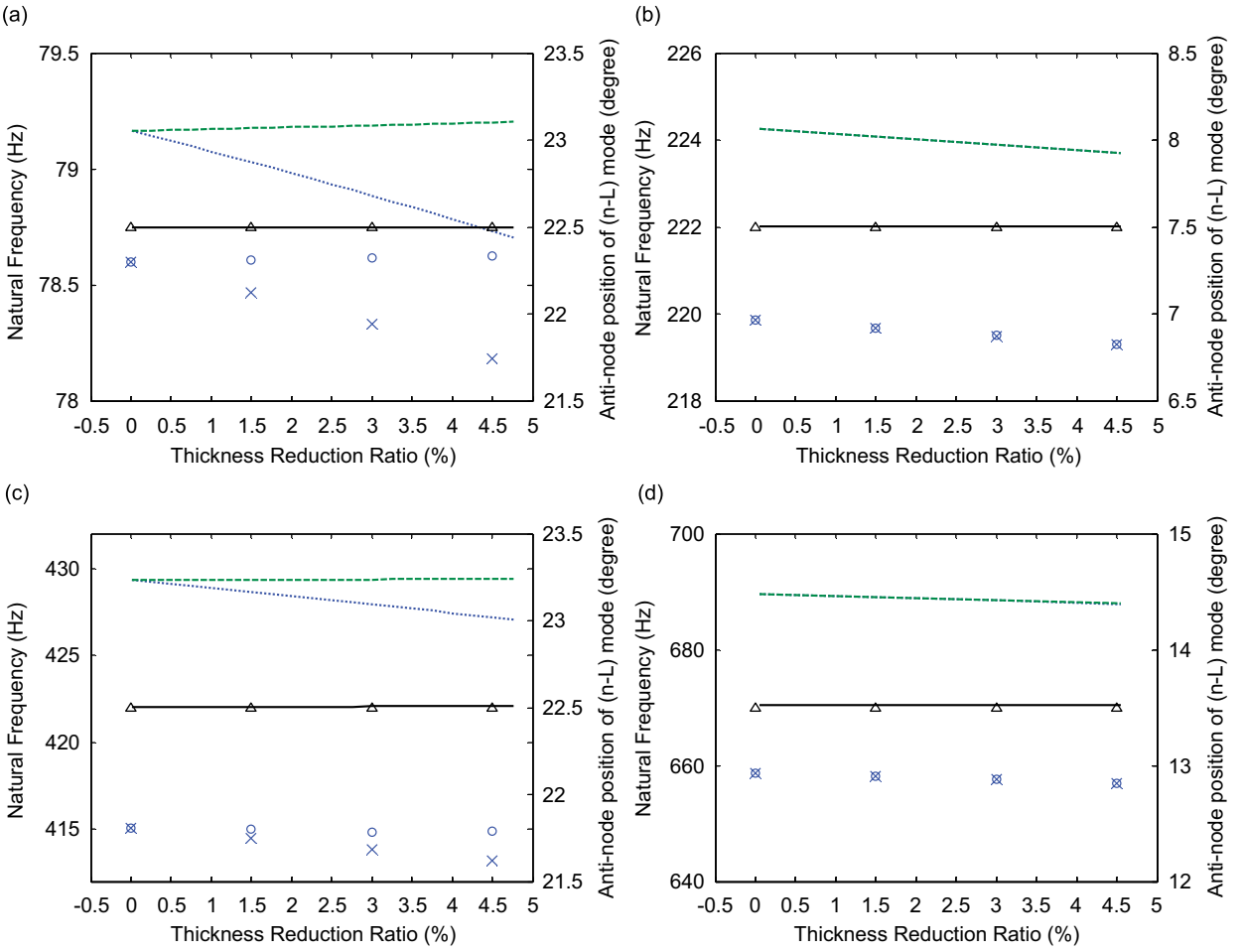

Fig. 7. Natural frequencies and anti-node position for two thickness elements (90° interval, deviations at $\theta = 22.5°, 112.5°$; $\Delta\theta_{1,2} = 9°$, $t_{1,2}$: 0–0.05t): (a) $n = 2$ mode; (b) $n = 3$ mode; (c) $n = 4$ mode; and (d) $n = 5$ mode. (– – (n–H)$_{\text{theory}}$, ····: (n–L)$_{\text{theory}}$, —: anti-node position of (n–L)$_{\text{theory}}$, ○: (n–H)$_{\text{FEM}}$, X: (n–L)$_{\text{FEM}}$, △: anti-node position of (n–L)$_{\text{FEM}}$).

thickness element. Coincidence of Figs. 6(a) and 7(a) reflects this situation, where Fig. 6(a) is plotted within the 10% range of the thickness reduction ratio and Fig. 7(a) within the 5% range. Same effect is available by the thickness reduction at every 90° from 22.5°. This situation is the same in the $n = 4$ mode with the same reason. From the result, we can expect the same change of the beat frequency by using multiple thickness elements with a small cut. But in $n = 3$ and 5 modes, one of the two thickness elements becomes a node and the other becomes an anti-node or vice versa, therefore the thickness effect by each element cancels. As a result the L and H mode pairs have the same frequency, as shown in Fig. 7(b) and (d).

We considered another case of two thickness elements, in which the thickness reduction was given at 22.5° and 82.5°. Because the two elements are 60° apart from each other, both elements become the anti-node of the L mode (node of H mode) in the $n = 3$ modes. Therefore, for the $n = 3$ modes, the frequency shift by the two thickness elements is double that of the one element case. Figs. 6(b) and 8(b) show this effect. Figs. 6–8 show that effect by two local stiffness deviations is almost the same between the theoretical method and the finite element analysis.

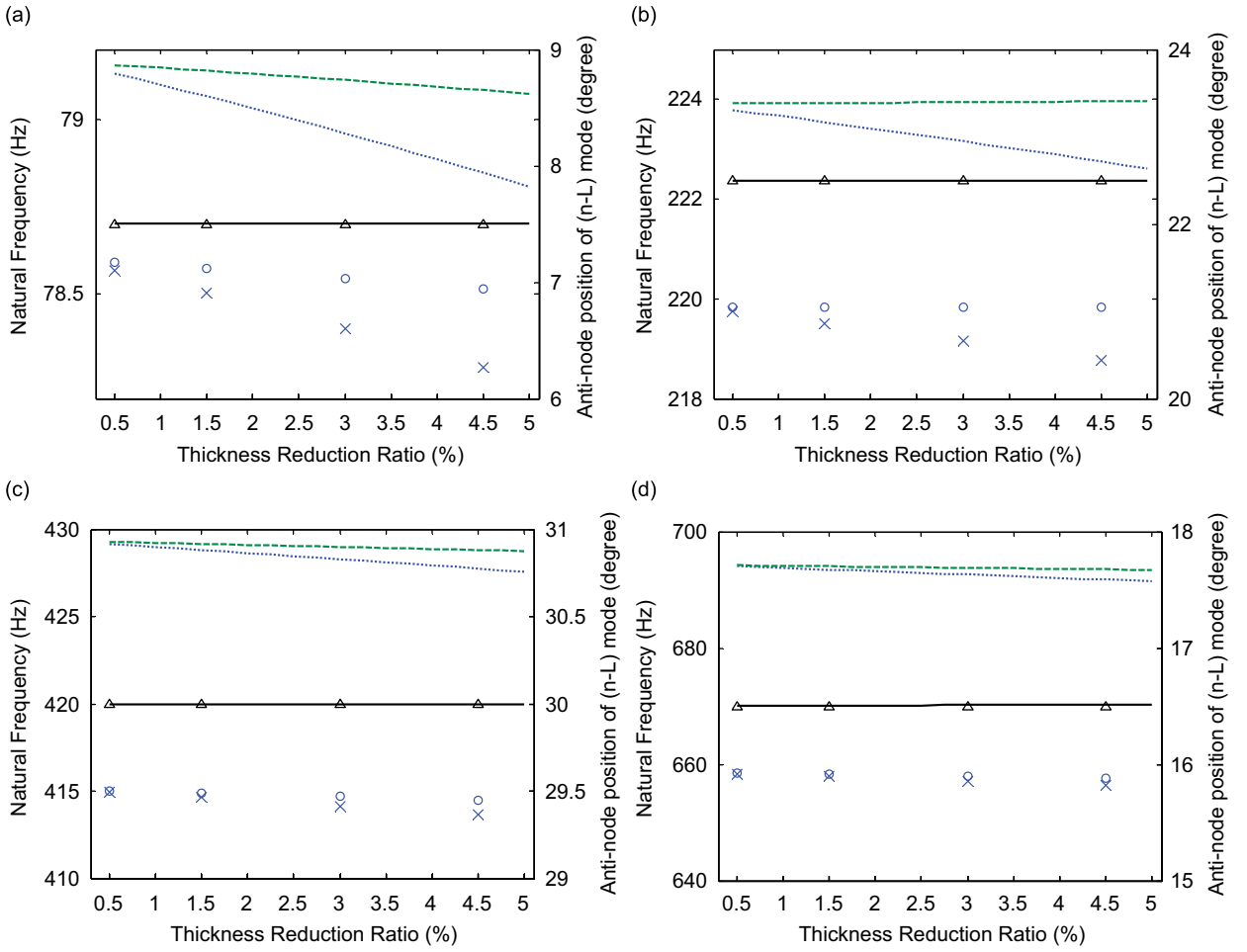

Fig. 8. Natural frequencies and anti-node position for two thickness elements (60° interval, deviations at $\theta = 22.5°, 82.5°$; $\Delta\theta_{1,2} = 9°$, $t_{1,2}$: 0–0.05t): (a) $n = 2$ mode; (b) $n = 3$ mode; (c) $n = 4$ mode; and (d) $n = 5$ mode. (– – (n–H)$_{\text{theory}}$, ····: (n–L)$_{\text{theory}}$, —: anti-node position of (n–L)$_{\text{theory}}$, ○: (n–H)$_{\text{FEM}}$, X: (n–L)$_{\text{FEM}}$, △: anti-node position of (n–L)$_{\text{FEM}}$).

4. Conclusions

Using the Laplace transform method and multiple heavy side step function, frequency shift in a mode pair of a circular ring with multiple local deviations was analyzed. Frequency shift in the n-L and n-H mode pair was investigated according to the change of locally distributed mass, stiffness and thickness non-uniformity. For the ring, as a simplified model of a large Korean bell, the natural frequencies of $n = 2$ and 3 modes agreed very well with those by the finite element analysis. Frequency shift in all mode pairs showed similar pattern between the theoretical analysis and the finite element analysis. Thickness reduction at the 22.5° element caused the anti-node of 2-L mode to pass the element and anti-node of 2-H mode to pass the −22.5° position. As a result, striking 0° equally excited the 2-L and 2-H mode pairs, and a clear beat was generated. The same effect was obtained by using multiple thickness elements. Thickness reductions at the 22.5° position and at 112.5° position produced the same effect on the mode pair. Same effect by the thickness reduction was produced at every 90° from 22.5°. Therefore, applying multiple small cuts, the beat characteristics can be controlled with a diminished fault effect. This type of beat control is available mode by mode by properly positioning the multiple cuts.

Acknowledgement

This work has been supported by the Institute of Advanced Machinery and Design in Seoul National University.

References

[1] R. Perrin, T. Charnley, G.M. Swallowe, On the tuning of church and carillon bells, *Applied Acoustics* 46 (1995) 83–101.
[2] J.M. Lee, S.H. Kim, S.J. Lee, J.D. Jeong, H.G. Choi, A study on the vibration characteristics of large size Korean bell, *Journal of Sound and Vibration* 257 (2002) 779–790.
[3] D. Allaei, W. Soedel, T.Y. Young, Natural frequencies and modes of rings that deviate from perfect axisymmetry, *Journal of Sound and Vibration* 111 (1) (1986) 9–27.
[4] Z. Cerep, In-plane vibrations of circular rings on tensionless foundation, *Journal of Sound and Vibration* 143 (3) (1990) 461–471.
[5] R.E. Rossi, In-plane vibration of circular rings of non-uniform cross-section with account taken of shear and rotatory inertia effects, *Journal of Sound and Vibration* 135 (3) (1989) 443–452.
[6] J.S. Hong, J.M. Lee, Vibration of circular ring with local deviation, *Transactions of the ASME, Journal of Applied Mechanics* 61 (1994) 317–322.
[7] S.H. Kim, W. Soedel, J.M. Lee, Beat characteristics of a bell type structure, *Journal of Sound and Vibration* 173 (1994) 517–536.
[8] S.H. Kim, C.W. Lee, J.M. Lee, Beat characteristics and beat maps of the King Seong-deok divine bell, *Journal of Sound and Vibration* 281 (2005) 21–44.
[9] W. Soedel, Vibration of shells and plates.